Chapter 4

Role of Ion Beam Excitations on Quasi One-Dimensional Magnetic system of Mn-doped $LiCuVO_4$

4.1 Introduction

The discovery of low-dimensional magnetic sub-systems, in complex metal oxides, has influenced the interest in these inorganic systems.[1-5] It gives us an insight to a variety of new quasi-one- and quasi-two-dimensional compounds, as well as systems of intermediate dimension- coupled magnetic chains or spin ladders. Such compounds are distinguished by specific temperature dependences of the magnetic properties and shows magnetic ordering at quite low temperatures. In fact, in certain cases, magnetic ordering does not occurs at all and one or another interaction mechanism opens up a spin gap in the magnetic excitation spectrum of a low-dimensional magnet.[6,7] The magnetic properties of most of low-dimensional magnets are governed by the presence of copper ions Cu^{2+} or vanadium ions V^{4+} in their structure. But, if these ions coexist with lithium ions Li^{1+}, then systems show most diverse variations of low-dimensional magnetic structures. Thus, in lithium cuprate $LiCuO_2$ the copper ions Cu^{2+} (S = 1/2) in linear CuO_4 chains are bound with one another by a ferromagnetic interaction, while the interaction between chains is antiferromagnetic.[8] Magnetic V^{4+} (S = 1/2) and nonmagnetic V^{5+} (S = 0) ions are present in the layered structure of lithium vanadate LiV_2O_5, and each of the ions form zig-zag chains of vanadium pyramids VO_5.

$LiCuVO_4$ is an important model material in quantum and frustrated magnetism. It is one of the best known realizations of the frustrated ferromagnetic chain where ferromagnetic nearest-neighbour interactions compete with next-nearest-neighbour interactions. This material attracts a lot of experimental and theoretical interest because of the plethora of quantum many-body phenomena it displays.[9-16] This ranges from fractional excitations, ferroelectricity and exotic high-magnetic field phases.[17-21] $LiCuVO_4$ is an orthorhombic system, which is genetically related to the spinel structure, having Li^{1+} and magnetic Cu^{2+} (S = 1/2) cations on octahedral sites and non-magnetic V^{5+} (S = 0) cations on tetrahedral sites.[2] Crystallographic structure of $LiCuVO_4$ contains two CuO_2 chains per unit cell running along b-axis.[3,4] There exists a competition between ferromagnetic nearest neighbor (NN) interaction and antiferromagnetic next nearest neighbor (NNN) interaction, within the chain. Antiferromagnetic NNN interaction dominates over ferromagnetic NN interaction and the system behaves like antiferromagnetic material. [22-31] Recently, the ion beam irradiation treatment of magnetic materials (CoPtCr, Fe-Pt, Ni-Fe, etc., having special relevance for application in magnetic information storage) have opened the renewed prospects of tailoring the

magnetic properties (e.g., moment, anisotropy, coercivity, magnetoresistance, etc.) which are significant for application purposes.[32-35] When swift heavy ions (SHI) incident on the material, it either excites or ionizes the atoms of the target by inelastic collisions or displaces them by elastic collisions. Elastic collision process is dominant in low-energy regimes and inelastic collision process dominates in high-energy regimes. It is evident from the literature that the electronic energy loss due to inelastic collision is capable of generating point or cluster defects if it is less than the threshold value of electronic energy loss. Stress (or strain) developed due to the created defects or amorphization is responsible for the modification of the materials.[36-38]

In this paper, we have studied the effect of doping of Mn in Cu site. Mn^{2+} with strong spin (S = 5/2) in comparison with Cu^{2+} (S = 1/2) looks promising to increase the ferromagnetic contribution in the competition. We have also studied the radiation effect on the magnetic and Raman scattering of Mn-doped $LiCuVO_4$ compound.

4.2 Experimental

The polycrystalline samples of $LiCu_{1-x}Mn_xVO_4$ (where x = 0.00, 0.05 and 0.10) were prepared by solid-state reaction from high purity Li_2CO_3, CuO, V_2O_5, and MnO powders. Powders were taken in stoichiometric ratio and mixed. The mixture was ground and pressed into pellets. Pellets were sintered at 550 ^{0}C for 48 hours with intermediate grindings. The X-ray powder diffraction has been taken from Rigaku MiniFlex II DEXTOP X-ray Diffractometer with Cu-kα radiation. Magnetic measurement was done using MPMS SQUID (Quantum Design) magnetometer.

The Ag ion irradiation has been performed at room temperature using 15UD Pelletron at Inter University Accelerator Centre (IUAC), New Delhi, India. The samples were mounted on a vacuum shielded vertical sliding copper ladder having four rectangular faces. The ion beam was magnetically scanned over an area of sample surface in a uniform way under high vacuum ~$6x10^{-6}$ torr. The beam current of ~0.4 pnA (particle nano Ampere) was maintained during irradiation. We have used three fluences, 5×10^{11} ions/cm^2 (1F), 1×10^{12} ions/cm^2 (2F) and 5×10^{12} ions/cm^2 (3F) of Ag^{11+} ion beam with energy 150 MeV.

4.3 Results and Discussion

4.3.1 X-ray Diffraction Study

Fig. 4.1 shows the X-ray diffraction (XRD) patterns of pristine and irradiated $LiCu_{1-x}Mn_xVO_4$ systems (where x = 0.00, 0.05 and 0.10). X-ray diffraction patterns have been refined with space group Imma with Li (4d) (1/4 1/4 3/4); Cu (4a) (0 0 0); V (4e) (0 1/4 z); O1 (8h) (0 y z); O2 (8i) (x 1/4 z). All observed peak positions of $LiCu_{1-x}Mn_xVO_4$ corresponds to standard Bragg positions of $LiCuVO_4$ (space group Imma), which have been shown by the red vertical bars, while the difference of observed intensities and calculated intensities have been shown as blue horizontal lines at the bottom of the XRD patterns in Fig. 4.1.

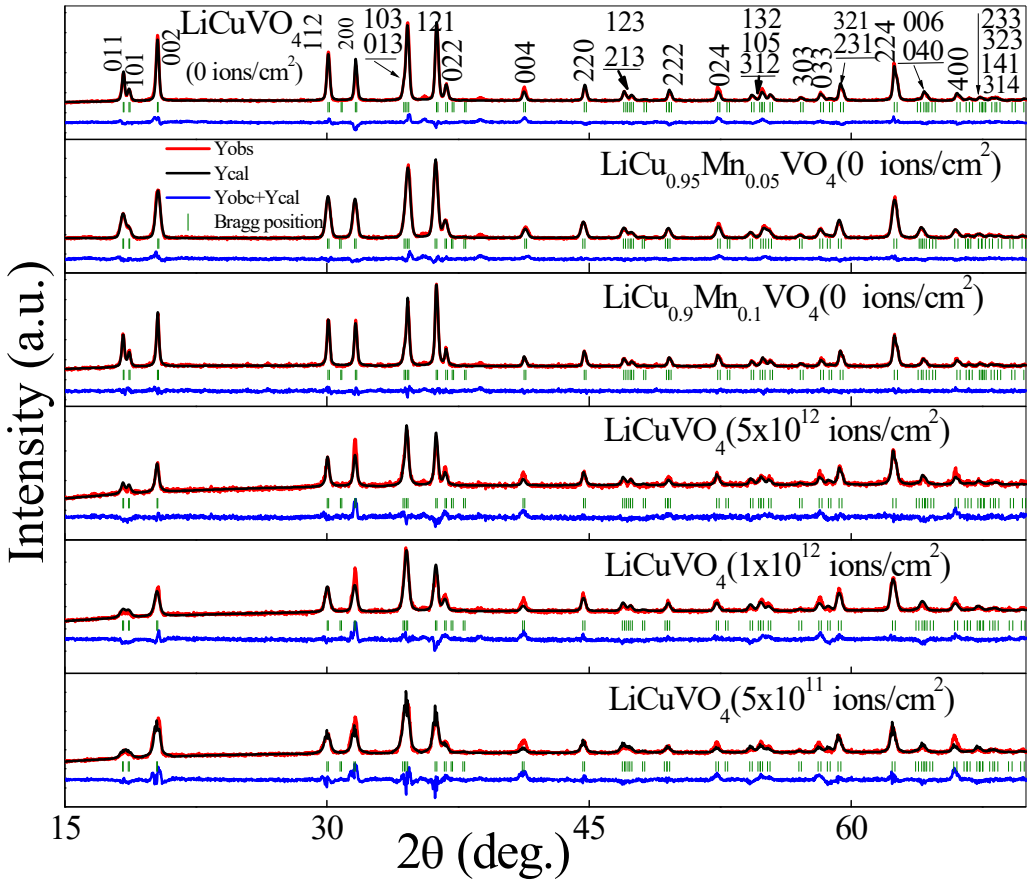

Fig. 4.1: *Rietveld refinement of X-ray diffraction pattern of $LiCu_{1-x}Mn_xVO_4$ (where x= 0.00, 0.05 and 0.10) and Irradiated $LiCuVO_4$ (2 F and 3F) with space group IMMA.*

The analysis of patterns confirm that all these $LiCu_{1-x}Mn_xVO_4$ systems have been crystallized in orthorhombic Imma space group and no trace of other impurities have been found. Lattice parameters obtained from refinement have been summarized in Table 4.1.

Lattice strain developed with the doping of Mn in Cu site, causes lattice parameter 'a' and 'b' to increase while 'c' decreases. With further increase of Mn in Cu site lattice parameters follow the same trend. Consequently, it has been observed that volume of the unit cell becomes larger with Mn doping. Another important fact to be noticed is that with irradiation, the irradiated materials' XRD peaks become broader than those of the pristine, which increases further with fluence values. Broadening of peak is due to formation of the smaller grain size with the irradiation. The lattice expansion in the irradiated samples can be explained on the basis of energy deposition mechanism in the irradiation process which demonstrate that the high electronic excitations have induced the structural modifications.[39-42]

Table 4.1: *Variation in lattice parameter of $LiCu_{1-x}Mn_xVO_4$ (x = 0.00, 0.05, 0.10) and irradiated $LiCuVO_4$. Reitveld Refinement has been done with Space group IMMA, Li (4d) (1/4 1/4 3/4); Cu (4a) (0 0 0); V (4e) (0 1/4 z); O1 (8h) (0 y z); O2 (8i) (x 1/4 z).*

Sample/ → Parameter ↓	$LiCuVO_4$ (0F)	$LiCu_{0.95}Mn_{0.05}VO_4$ (0F)	$LiCu_{0.9}Co_{0.1}VO_4$ (0F)	$LiCuVO_4$ (1F)	$LiCuVO_4$ (2F)	$LiCuVO_4$ (3F)
a (Å)	5.6530 (2)	5.6542 (7)	5.6536 (3)	5.6670 (4)	5.6641 (6)	5.6607 (6)
b (Å)	5.8009 (3)	5.8030 (3)	5.8047 (3)	5.8112 (4)	5.8110 (6)	5.8078 (6)
c (Å)	8.7464 (4)	8.7446 (5)	8.7414 (5)	8.7614 (8)	8.7582 (10)	8.7554 (10)
Volume	286.813 (0.023)	286.870 (0.026)	286.925 (0.015)	288.536 (0.039)	288.268 (0.054)	287.842 (0.052)
V (4e) z	0.6135 (10)	0.6116 (5)	0.6134 (5)	0.6095 (9)	0.6177 (7)	0.6159 (8)
O1 (8h) y	0.5084 (12)	0.5038 (14)	0.5147 (13)	0.4730 (3)	0.4900 (2)	0.4950 (2)
z	0.2875 (8)	0.2919 (9)	0.2749 (7)	0.3013 (18)	0.2966 (12)	0.2868 (12)
O2 (8i) x	0.2321 (8)	0.2305 (9)	0.2329 (10)	0.2130 (2)	0.2163 (17)	0.2190 (2)
z	0.0006 (8)	0.0011 (9)	0.0013 (9)	0.0020 (2)	0.0113 (17)	0.0090 (2)
Distances/angles						
(Cu-O1)x2	2.515 (7)	2.553 (8)	2.405 (11)	2.644 (16)	2.598 (11)	2.511 (11)
(Cu-O2)x4	1.956 (3)	1.950 (3)	1.961 (8)	1.889 (7)	1.903 (6)	1.911 (7)
(V-O1)x2	1.647 (7)	1.660 (14)	1.686 (15)	1.790 (15)	1.688 (17)	1.709 (19)
(V-O2)x2	1.808 (5)	1.805 (15)	1.806 (18)	1.898 (19)	1.965 (12)	1.931 (12)
O1-Cu-O2	89.0 (4)	89.9 (4)	88.5 (4)	86.9 (9)	86.0 (6)	87.1 (7)
O2-Cu-O2	84.3 (3)	83.9 (3)	84.0 (4)	79.4 (7)	80.2 (6)	80.9 (7)
O1-V-O2	106.7 (5)	105.7 (6)	108.5 (5)	103.0 (11)	104.8 (9)	106.4 (10)
O1-V-O1	116.6 (7)	120.6 (8)	108.8 (7)	128.2 (16)	127.2 (11)	120.2 (11)
O2-Li-O1	82.8 (4)	81.7 (4)	86.3 (4)	80.9 (9)	82.1 (7)	84.2 (8)
O1-Li-O1	88.1 (2)	89.7 (5)	86.4 (2)	82.2 (11)	86.8 (7)	88.9 (7)
R_{wp}	17.8	18.9	19.2	36.4	32.7	35.1
χ^2	3.54	3.83	3.73	7.58	4.89	3.40

4.3.2 Jahn-Teller Distortion

Cu^{2+} having $3d^9$ configuration, possess orbitally degenerate electronic configuration, is destined for Jahn-Teller distortion. Cu^{2+} cations exist in the $LiCuVO_4$ system in CuO_6 octahedral co-ordination. Out of six Cu-O bonds in octahedral co-ordination, four bonds exist in a-b plane (denoted as CuO_2) and two bonds directed along c-axis (denoted as Cu-O1). Cu-O1 bonds of CuO_6 octahedra present in $LiCuVO_4$ have been elongated due to Jahn-Teller effect along c-axis. With Mn doping this elongation along c-axis increases further but with further increase in Mn concentration, CuO_6 octahedra experiences a decrease in elongation as Cu-O1 bond-length decreases even below Cu-O1 bond-length of $LiCuVO_4$. Moreover. It is worthwhile to mention that Mn^{+3} is a Jahn-Teller distorted ion and therefore, if Mn doped $LiCuVO_4$, Mn is in 3+ state then, due to this Mn^{+3} the Jahn-Teller would be enormous. In the previous report[43] we have seen from the X-ray photoemission study that though Mn maintains the 2+ state when doped in $LiCuVO_4$ on Cu site, even then very small amount of Mn^{+3} exists. For the irradiated samples of undoped $LiCuVO_4$, it has been observed that for the 1F fluence lattice strain is maximum, causing the values of the lattice parameters maximum (values of a, b and c increase) and as the fluence increases to 2F and 3F, the lattice parameters decrease. Similarly, Jahn-Teller elongation of Cu-O1 bond is maximum for 1F fluence, with further increase of fluence to 2F and 3F, the Cu-O1 bond elongation reduces to initial elongation observed for pristine $LiCuVO_4$.

The Jahn-Teller distortion is usually described by parameters which are directly calculated from the structural data. The radial (ρ) and angular (ψ) Jahn-Teller distortion parameters are defined as;[44, 45]

$$\rho = 2^{1/2}\,[(\Delta u)^2 + (\Delta v)^2 + (\Delta z)^2]^{1/2} \qquad (4.1)$$

$$\psi = 3^{1/2}\,(\frac{\Delta u - \Delta v}{2\Delta z - \Delta u - \Delta v}) \qquad (4.2)$$

In-plane bond distances in $LiCuVO_4$

$$d_{av} + \Delta u = 1.956\ A^{\circ}\ (\times 2) \qquad (4.3)$$

$$d_{av} + \Delta v = 1.956\ A^{\circ}\ (\times 2) \qquad (4.4)$$

Out of plane bond distances in $LiCuVO_4$

$$d_{av} + \Delta z = 2.515\ A^{\circ}\ (\times 2) \qquad (4.5)$$

Where 1.956 A° and 2.515 A° represent values of Cu-O2 and Cu-O1 bond-lengths (in angstrom) respectively, of $LiCuVO_4$.

Average Cu-O bond distance, [44]

$$d_{av} = 2.120\ A° \ (\times 6) \qquad (4.6)$$

Jahn-Teller distortion parameters of doped and irradiated systems calculated from equation (1) and (2) have been shown in Fig. 4.2. Radial Jahn-Teller distortion (ρ) parameter first increases and then decreases with Mn doping. However, when $LiCuVO_4$ have been irradiated with 1F fluence, Jahn-Teller distortion increases while with further increase of fluence to 2F and 3F the Jahn-Teller distortion decreases. With further increase of fluence to 2F and 3F (means increase of ion bombardment duration) the system shows decrease in Jahn-Teller distortion. When, these heavy ions (Ag^{11+}) incident on the system's surface, they penetrate the surface to some extent. Due to the sudden entrance of Ag ions the crystal symmetry changes for the sake of adjustment to the ghost ions, which might be the reason of increase in Jahn-Teller distortion. With increase of duration of ion bombardment there is no further increase in defects and system starts to normalize itself, this is evident from the decrease in Jahn-Teller distortion.

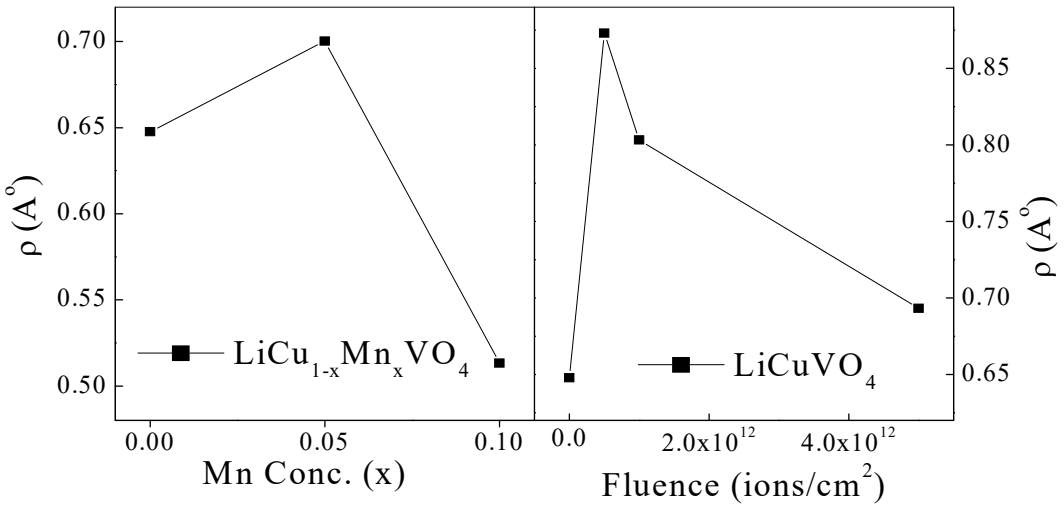

Fig. 4.2: *(a) Variation of Jahn-Teller distortion (ρ) for $LiCu_{1-x}Mn_xVO_4$ (where x =0.00, 0.05 and 0.10) and (b) variation of Jahn-Teller distortion for $LiCuVO_4$ with respect to irradiation fluence.*

4.3.3 Raman Spectroscopy Study

To get the information about local structural changes occurred in the system due to doping and irradiation, Raman spectra of all the doped and irradiated samples have been analyzed. Raman spectra of pristine $LiCu_{1-x}Mn_xVO_4$ systems are shown in Fig. 4.3. The observed Raman modes can be categorized into three different frequency range of lattice vibrations. In the high-frequency range (650-1000cm^{-1}), the vibration mode is the stretching of the distorted VO_4 groups. In this range, we expect stretching modes ν_1 and ν_3 of the distorted VO_4 groups. Vibration ν_3 is triply degenerate, which splits into three modes: A_g, B_{2g} and B_{3g}. Vibration ν_1 is non-degenerate and it transforms into the A_g mode in the crystal.[46]

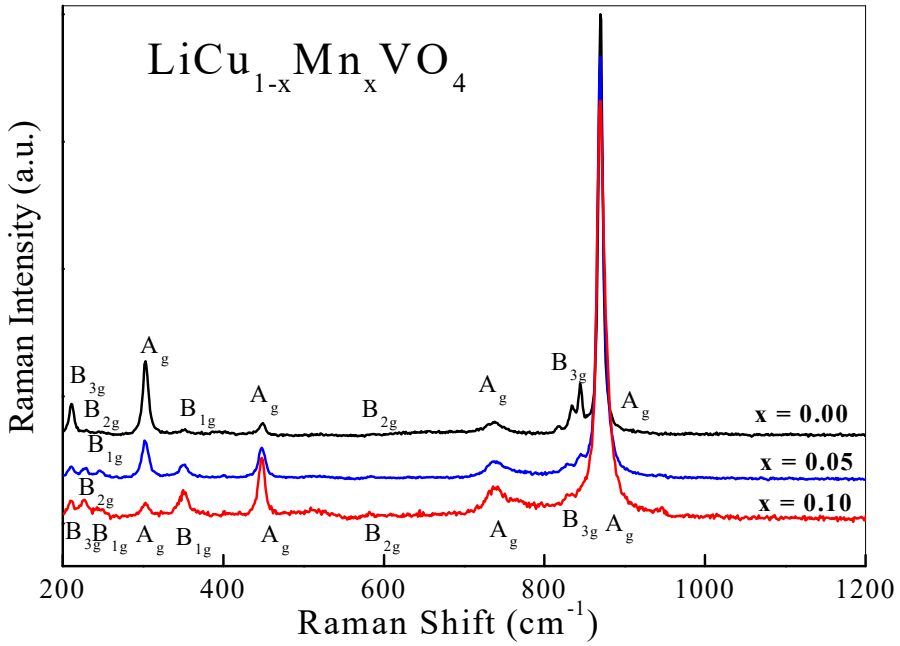

Fig. 4.3: *Raman spectra of $LiCu_{1-x}Mn_xVO_4$ system.*

Therefore, four peaks of Raman spectra ($2A_g+B_{2g}+B_{3g}$) in high frequency range correspond to the stretching V–O_1 and V–O_2 vibration. In the intermediate-frequency (400-650 cm^{-1}) range, the peaks are often related to complex vibrations, involving the simultaneous participation of all cations, tetrahedral and octahedral.[47] Bands with frequencies below 400 cm^{-1} can be assigned to complex vibrations with a predominant contribution of the Li^+ and Cu^{2+} cations. With doping of Mn in $LiCuVO_4$, for x=0.05 the peak width decreases slightly (indicative of increase of strain) and as Mn content

increases (viz. for x=0.1) the peak broadens indicating the release of strain with increase of Mn contents which is consistent with the XRD analysis. Other than this no significant change is observed in the Raman modes of the system.

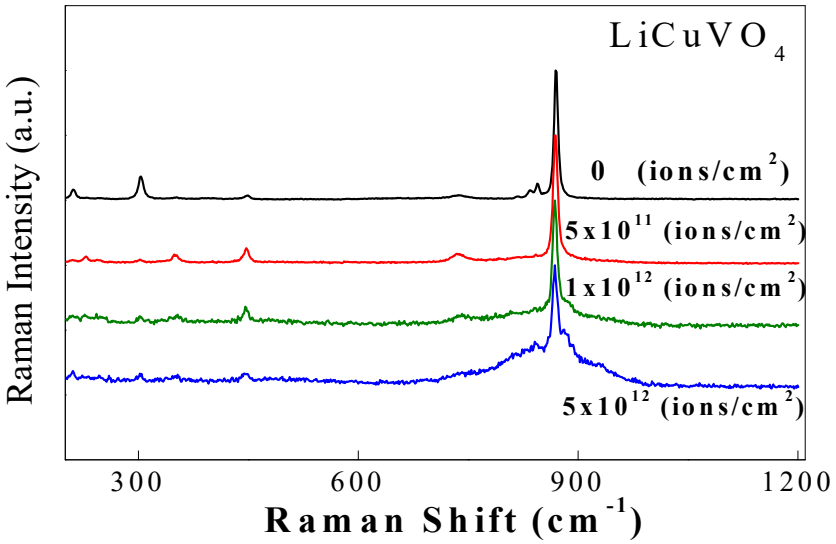

Fig. 4.4: *Raman spectra of non-irradiated and irradiated $LiCuVO_4$ with 1 F, 2F and 3 F fluencies.*

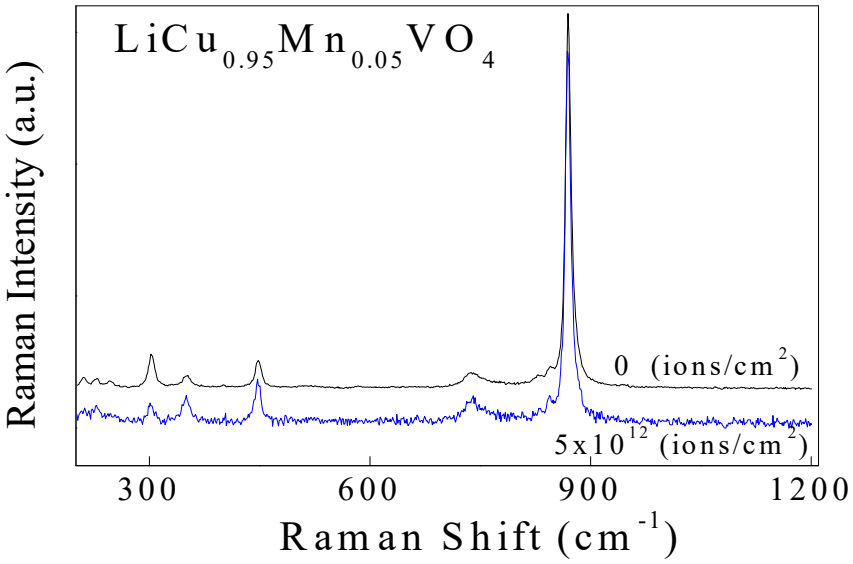

Fig.4.5: *Raman spectra of non-irradiated and irradiated $LiCu_{0.95}Mn_{0.05}VO_4$ with 3 F fluence.*

We have also studied the effect of irradiation on the Raman modes of undoped (Fig. 4.4) and doped $LiCuVO_4$ samples (Figs. 4.5 & 4.6). It has been observed that in undoped $LiCuVO_4$ there is no appreciable change in low and intermediate frequency regions due to irradiation but bands in high frequency region has been distorted and distortion

increases with increasing irradiation time, which might be due to the local distortion occurred in the system due to irradiation. These observed broadening in Raman modes with increasing irradiation fluence suggests the release of strain in the system, which is in conformation of the XRD study.

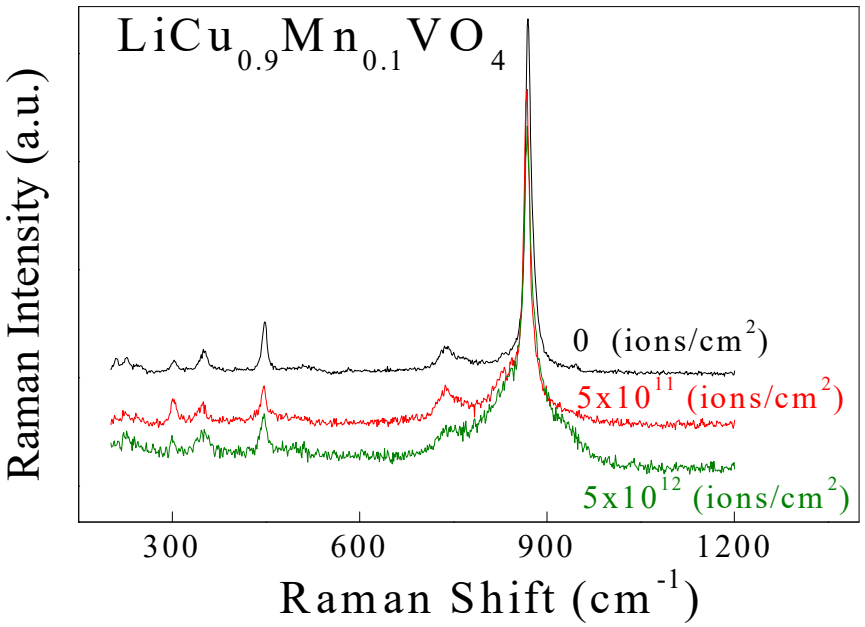

Fig.4.6: *Raman spectra of non-irradiated and irradiated $LiCu_{0.9}Mn_{0.1}VO_4$ with 1 F and 3 F fluencies.*

4.3.4 Magnetization Measurements

Modifications observed in the structure of the irradiated samples, as revealed by XRD and Raman spectra, would immensely affect the magnetic properties of $LiCu_{1-x}Mn_xVO_4$. Thermal variation of magnetizations has been shown in Fig.4.7. It can be seen for $LiCuVO_4$ that with lowering temperature, magnetization increases steadily and it exhibits a broad peak around 27 K. With further decrement in temperature, magnetization shows a dip in magnetization and starts increasing again near 13 K. It is a typical behavior of a quasi-1D magnet, which shows short range magnetic correlation within the chain as the temperature decreases and at very low temperature (for $LiCuVO_4$ it is 2.1K) attains 3-dimensional antiferromagnetic ordering. Our system does not show long range antiferromagnetic ordering because the lower temperature limit in our measurement is 5K. For $LiCu_{0.95}Mn_{0.05}VO_4$ system, magnetization increases very slowly with decrease

of temperature down to around 50 K and with further lowering of temperature magnetization sharply increases and exhibits a peak around 21 K.

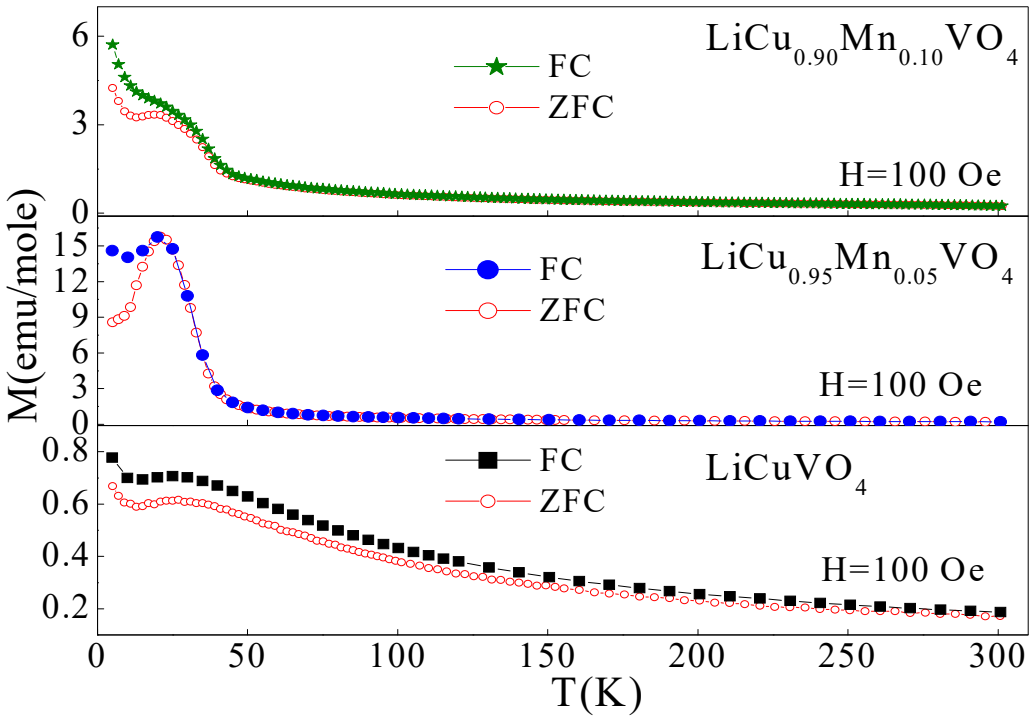

Fig.4.7: *Magnetization (M) vs Temperature (T) curve of $LiCu_{1-x}Mn_xVO_4$ (where x = 0.00, 0.05 and 0.10) at 100 Oe.*

The magnetization value starts increasing after showing a dip around 10 K (like $LiCuVO_4$). But for $LiCu_{0.90}Mn_{0.10}VO_4$, increment in magnetization is not that sharp like $LiCu_{0.95}Mn_{0.05}VO_4$ and its value also decreases with respect to $LiCu_{0.95}Mn_{0.05}VO_4$ system but it remains higher in comparison to pure $LiCuVO_4$. In $LiCu_{0.90}Mn_{0.10}VO_4$ system, magnetization increases after showing a dip around 10 K. Fig. 4.8 shows the magnetization vs temperature curve at 1000 Oe. Except the increased magnetization values, behavior of all the samples is almost similar. Fig. 4.9 shows M-H hysteresis curve of $LiCu_{1-x}Mn_xVO_4$ system (where x= 0.00, 0.05 and 0.10) at 5K. $LiCuVO_4$ shows a linear M-H curve which is due to the antiferromagnetic nature of the system. But both Mn doped systems show non-linear M-H hysteresis curve and show enhanced magnetization. At higher field, with Mn doping magnetization value is increasing. But at low field, magnetization of $LiCu_{0.95}Mn_{0.05}VO_4$ is higher than $LiCu_{0.90}Mn_{0.10}VO_4$ (inset figure). Pure $LiCuVO_4$ does not show any coercivity but $LiCu_{0.95}Mn_{0.05}VO_4$ does. This implies that doping of Mn develops short range magnetic ordering in the system which enhances its magnetization. With further doping of Mn this magnetic ordering deteriorates which

results in decrement in coercivity and magnetization value. There is a competition between ferromagnetic nearest neighbor (NN) coupling and antiferromagnetic next nearest neighbor (NNN) coupling in CuO_2 chain.[2]

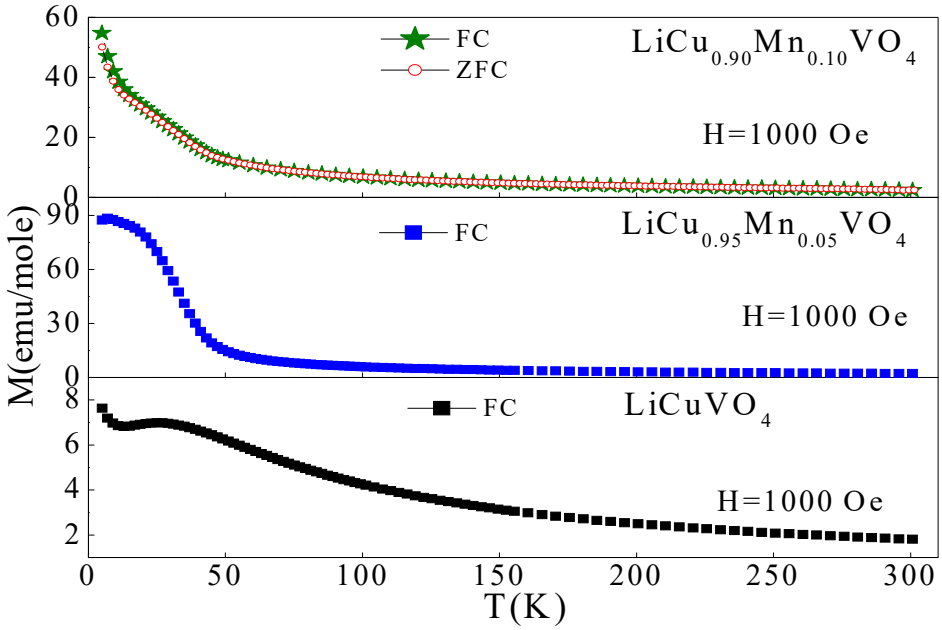

Fig. 4.8: *Magnetization (M) vs Temperature (T) curve of $LiCu_{1-x}Mn_xVO_4$ (where x = 0.00, 0.05 and 0.10) at 1000 Oe.*

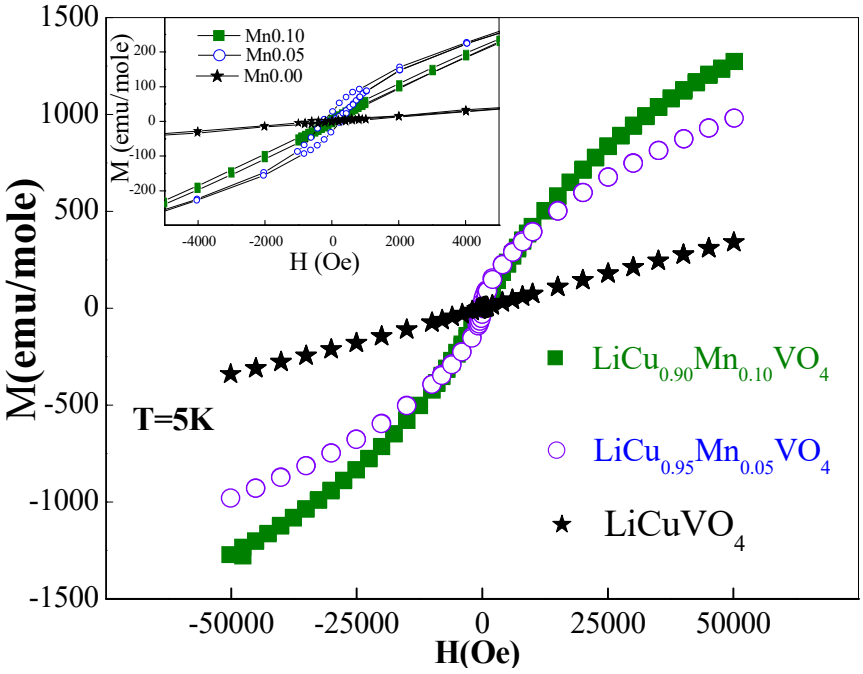

Fig. 4.9: *M-H hysteresis curve of $LiCu_{1-x}Mn_xVO_4$ (where x = 0.00, 0.05 and 0.10) at 5 K.*

In $LiCuVO_4$, NNN coupling dominates over NN coupling and resultantly system behaves as an antiferromagnet. With Mn doping, ferromagnetic NN coupling gets a slight edge over the antiferromagnetic NNN coupling, due to strong magnetic moment of Mn^{2+} in comparison to Cu^{2+}. As we have studied from the magnetic measurements that due to the doping of Mn in the $LiCuVO_4$ systems there occurs a short range magnetic ordering. Further doping of Mn in the system disturbs this short range ordering and system becomes less sensitive to low magnetic fields. But, at higher magnetic field its response to the field becomes better perhaps due to strong magnetic moment of Mn^{2+}. As has been discussed from XRD and Raman scattering study that for x=0.05 the strain is maximum, therefore, it might be the fact that strain changes the canting angle which may induce the short range ferromagnetic ordering. With increase of Mn content the strain is released and the system tends to its original state and the ferromagnetism decreases.

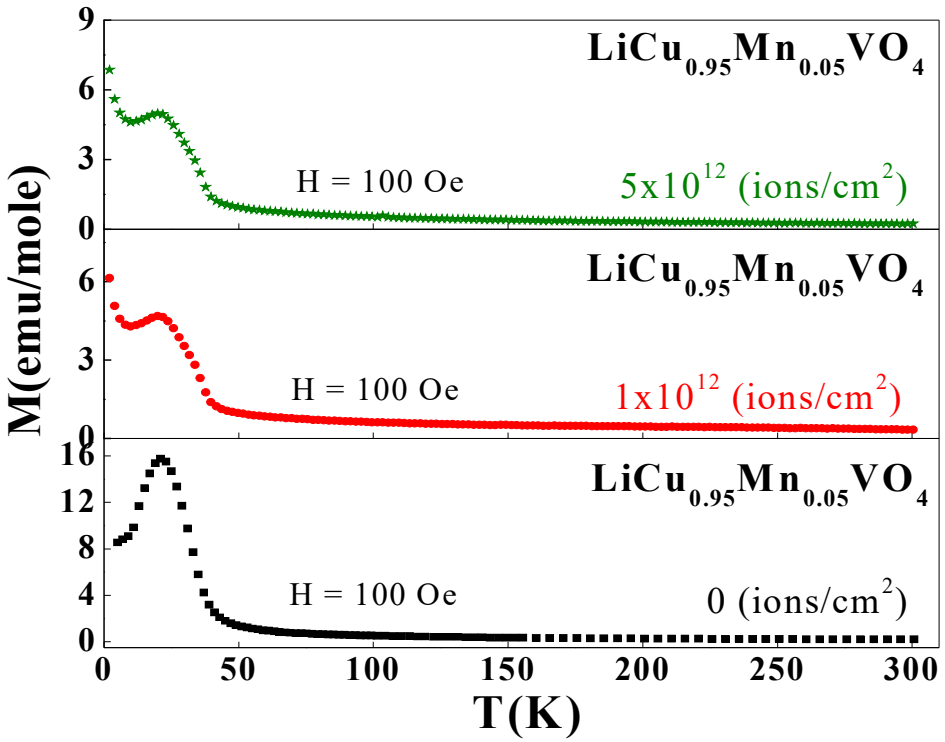

Fig. 4.10*: Irradiation effect on Magnetization (M) vs Temperature (T) curve of $LiCu_{0.95}Mn_{0.05}VO_4$ sample at 100 Oe.*

To investigate the effect of irradiation on the magnetic properties of the system, we have chosen the system with better magnetic response, i.e., $LiCu_{0.95}Mn_{0.05}VO_4$. We have irradiated the system with two fluencies 2F and 3F. Fig. 4.10 shows, magnetization curve of 0F, 2F and 3F samples. It can be seen that due to irradiation effect, magnetization

of the system degraded. Furthermore, there is no appreciable change observed in magnetization of the sample by varying the fluences. This means defects, which are produced on the surface of the sample, does not show any dependency on the time of exposure to the ion-beam. Fig. 4.11 shows M-H hysteresis loop for un-irradiated and irradiated $LiCu_{0.95}Mn_{0.05}VO_4$ sample. Hysteresis loops confirm that coercivity (which was induced due to Mn doping) have been diminished due to irradiation effect and the system is tending towards paramagnetic state, which is in quite support with the previous observations.[48-51] Defects created by the ion irradiation affects ferromagnetic NN coupling more in comparison to antiferromagnetic NNN coupling, because the ferromagnetic ordering induced by Mn is of short range and local defects created on the surface of the sample have more effect on short range ferromagnetic ordering rather than long range antiferromagnetic ordering.

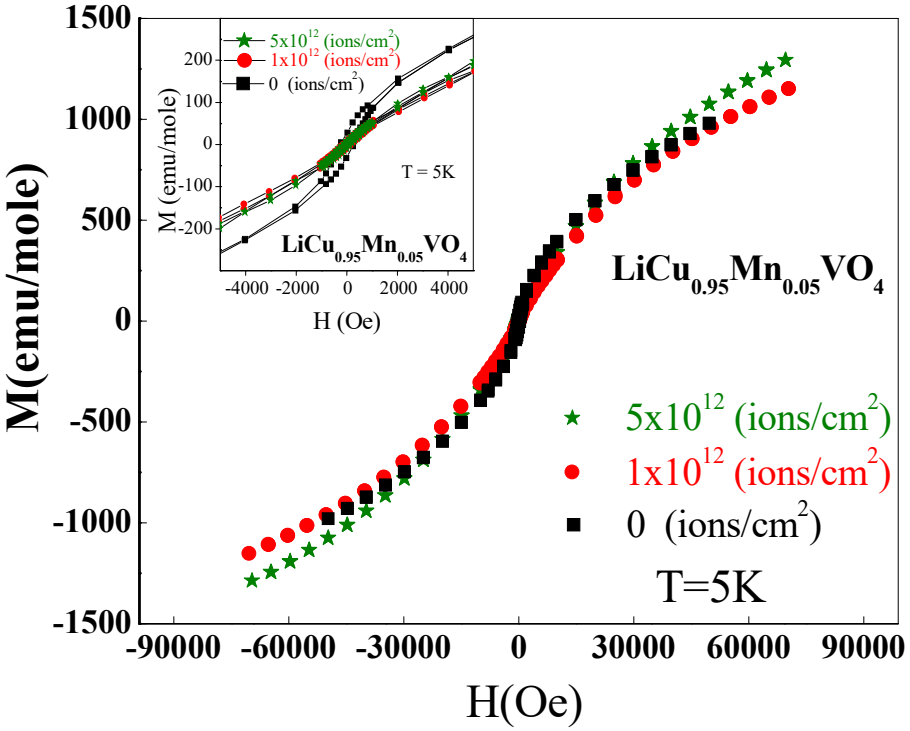

Fig. 4.11: *Irradiation effect on M-H hysteresis curve of $LiCu_{0.95}Mn_{0.05}VO_4$ at 5 K.*

The changeover in response of the magnetic Cu ion with doping of Mn and effect of irradiation is further illustrated in Fig. 4.12 for which the $\chi(T)T$ product is shown as a function of temperature. For temperature independent spins, and temperatures far above the effective interaction temperature, it is found that this product is temperature

independent. The χ(T)T value changes with doping of different transition metal ions indicating essentially change of interactions among the magnetic Cu ions. $LiCu_{0.95}Mn_{0.05}VO_4$ sample shows clear deviation from antiferromagnetic ordering and signature of ferromagnetism. A hump like behaviour is observed in χ(T) plot. This is usual for low-dimensional system and is associated with the appearance of the magnetic correlation within the copper chains. But for Mn-doped sample only a kink is observed. Moreover, if in both χ(T) and χT(T) plots peak is observed then it indicates the magnetic ordering.

For the un-doped sample neither in χ(T) plot nor in χT(T) plot any peak is observed within the measured temperature range. But in Mn-doped sample in both the curves peak is observed. Irradiation causes the decrement in peak intensity but ferromagnetic behaviour remains intact which supports what we have already mentioned.

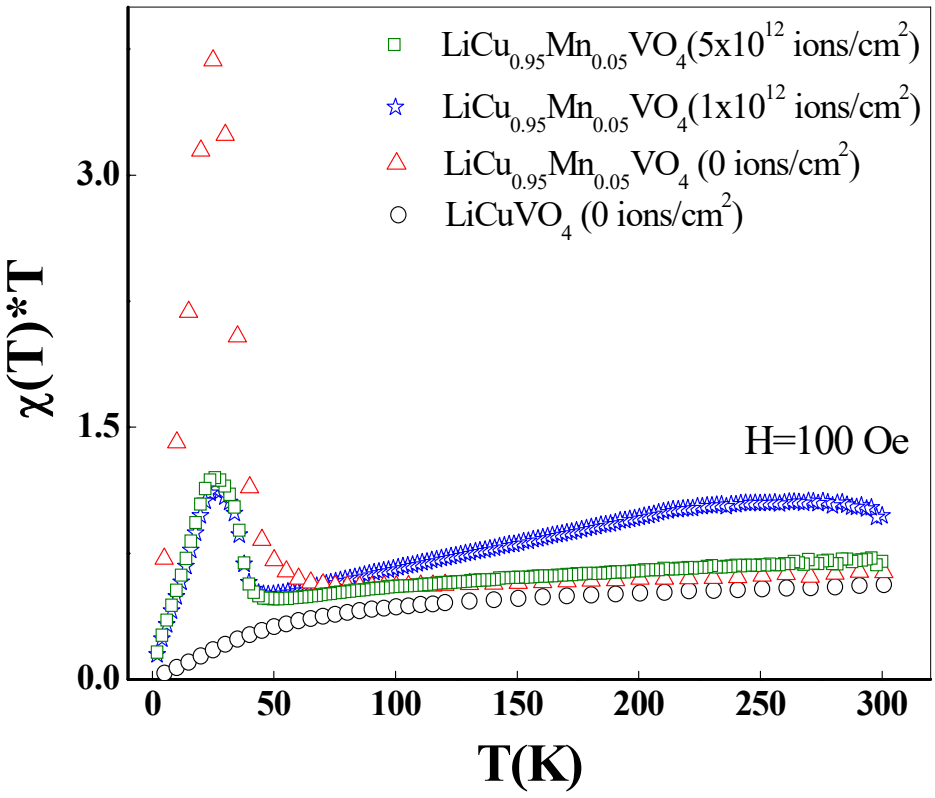

Fig.4.12: *χ(T)T as a function of temperature of $LiCuVO_4$, $LiCu_{0.95}Mn_{0.05}VO_4$, $LiCu_{0.95}Mn_{0.05}VO_4$ (2F), $LiCu_{0.95}Mn_{0.05}VO_4$ (3F) samples.*

4.4 Conclusion

X-ray diffraction results indicate that the pristine materials relaxes on irradiation. The irradiated materials' XRD peaks become broader than those of the pristine, which increases further with fluence values. Broadening of peak is due to the formation of the smaller grain size with the irradiation. The lattice expansion in the irradiated samples can be explained on the basis of energy deposition mechanism in the irradiation process which demonstrates that the high electronic excitations have induced the structural modifications. With doping of Mn in $LiCuVO_4$, no significant change is observed in the Raman modes of the system. For x=0.05 the peak width decreases slightly (indicative of increase of strain) and as Mn content increases (viz. for x=0.1) the peak broadens indicating the release of strain with increase of Mn contents which is consistent with the XRD result. Irradiation causes no change in Raman modes of $LiCu_{0.95}Mn_{0.05}VO_4$ system, while apparent peak broadening is observed in Raman spectra with increasing irradiation fluence which is the indicative of release of strain. A short range ferromagnetic ordering has been observed with the doping of Mn in the octahedral site of spinel $LiCuVO_4$ system. This short range ferromagnetic ordering is not stable as inclusion of further Mn decreases the coercivity of the system. The defects created by the Ag^{11+} ion beam irradiation might be affecting the short range ordering and hence reducing the ferromagnetic behavior.

References:

[1] Shengelaya, G.T. Meijer, J. Karpinski, Guo-meng. Zhao, H. Schwer, E.M. Kopnin, C. Rossel and H. Keller, Phys. Rev. Lett. **80,** 3626 (1998).

[2] S.A. Carter, B. Batlogg, R.J. Cava, J.J. Krajewski, J.R. Peck and T. M. Rice, Phys. Rev. Lett. **77,** 1378 (1996).

[3] A.A. Belik, M. Azuma and M. Takano, Inorg. Chem. **42**, 8572 (2003).

[4] E. Dagotto and T.M. Rice, Science **271,** 618 (1996).

[5] Z. Hiroi, S. Amelinckx, G. Van. Tendeloo and N. Kobayashi, Phys. Rev. B **54,** 15849 (1996).

[6] M. Hase, I. Terasaki and K. Uchinokura, Phys. Rev. Lett. **70,** 3651 (1993),

[7] M. Isobe and Y. Ueda, J. Phys. Soc. Jpn. **65**,1178 (1996).

[8] M. Boehm, S. Coad and S. Uchida Euro. Phys. Lett. **43**, 77 (1998).

[9] Y. Naito, K. Sato, Y. Yasui, Y. Kobayashi, Y. Kobayashi and M. Sato, J. Phys. Soc. Jpn. **76**, 023708 (2007).

[10] Ch. Kegler, N. Büttgen, H.A. Krug von Nidda, A. Krimmel, L. Svistov, B.I. Kochelaev, A. Loidl , A. Prokofiev and W. Abmus, Eur. Phys. J. B **22**, 321 (2001).

[11] H.A. Krug von Nidda, L.E. Svistov, M.V. Eremin, R.M. Eremina, A. Loidl, V. Kataev, A. Validov, A. Prokofiev and W. Assmus, Phys. Rev. B **65**, 134445 (2002).

[12] D. Dai, H.J. Koo and M.H. Whangbo, Inorg. Chem. **43,** 4026 (2004).

[13] N. Hur, S. Park, P. A. Sharma, J. S. Ahn, S. Guha and S. W. Cheong, Nature **429**, 392 (2004),

[14] M. Enderle, C. Mukherjee, Fak B, R.K. Kremer, J.M. Broto, H. Rosner, S.L. Drechsler, J. Richter, J. Malek, A. Prokofiev, W. Assmus, S. Pujol, J.L. Raggazzoni, H. Rakoto, M. Rheinsta¨dter and H.M. Rnnow, Euro phys. Lett. **70** 237 (2005).

[15] F. Schrettle, S. Krohns, P. Lunkenheimer, J. Hemberger, N. Büttgen, H.A.Krug von Nidda, A.V. Prokofiev and A. Loidl, Phys. Rev. B **77**, 144101 (2008).

[16] L.E. Svistov, T. Fujita, H. Yamaguchi, S. Kimura, K. Omura, A. Prokofiev, A.I. Smirnov, Z. Honda and M. Hagiwara, JETP Lett **93**, 21 (2011).

[17] T. Fujita, M. Hagiwara, H. Yamaguchi, S. Kimura, L.E. Svistov, A.I. Smirnov and A. Prokofiev, J. Phys. Soc. Jpn. **81** ,SB029 (2012).

[18] M. Mourigal, M. Enderle, R.K. Kremer, J.M. Law and B. Fak, Phys. Rev. B **83** 100409 (2011)

[19] M. Mourigal, M. Enderle, B. Fak, R.K. Kremer, J.M. Law, A. Schneidewind,A. Heiss and A. Prokofiev, Phys. Rev. Lett. **109**, 027203 (2012).

[20] T. Masuda, M. Hagihala, Y. Kondoh, K. Kaneko and N. Metoki, J. Phys. Soc Jpn. **80**,113705 (2011).

[21] Nawa Kazuhiro, Takigawa Masashi, Yoshida Makoto and Yoshimura Kazuyoshi J. Phys. Soc. Jpn. **82**, 094709 (2013).

[22] S.L. Drechsler, J. Richter, R. Kuzian, J. Málek, N. Tristan, B. Büchner, A.S. Moskvin, A.A. Gippius, A. Vasilievf, O. Volkovaf, A. Prokofievg, H. Rakotoh, J.M. Brotoh, W. Schnelle, M. Schmitt, A. Ormeci, C. Loisoni and H. Rosner, J. Mag. Mag. Mat **316**, 306 (2007).

[23] M. Mostovoy, Phys. Rev. Lett. **96** ,067601 (2006).

[24] S. Nishimoto, S.L. Drechsler, R. Kuzian, J. Richter, J. Málek, M. Schmitt, J.V.D. Brink and H. Rosner, Euro. Phys. Lett. **98** , 37007(2012).

[25] T. Hikihara, L. Kecke, T. Momoi and A. Furusaki, Phys. Rev. B **78,** 144404 (2008).

[26] J. Sudan, A. Luscher and A.M. Lauchli, Phys. Rev. B **80**, 140402 (2009).

[27] M. Sato, T. Momoi and A. Furusaki, Phys. Rev. B **79**, 060406 (2009).

[28] M. E. Zhitomirsky and H. Tsunetsugu, Europhys. Lett. **92** ,37001 (2010).

[29] M. Sato, T. Hikihara and T. Momoi, Phys. Rev. B **83,** 064405 (2011).

[30] S. Furukawa, M. Sato, S. Onoda and A. Furusaki, Phys. Rev. B **86,** 094417 (2012)

[31] M. Sato, T. Hikihara and T. Momoi, Phys. Rev. Lett. **110,** 077206 (2013).

[32] R. Allenspach, A. Bischof, U. Dürig and P. Grütter, Appl. Phys. Lett. **73,** 3598 (1998).

[33] G.S. Chang, T.A. Callcott, G.P. Zhang, G.T. Woods, S.H. Kim, S.W. Shin, K. Jeong, C.N. Whang and A. Moewes, Appl. Phys. Lett. **81,** 3016 (2002).

[34] O. Hellwig, D. Weller, A.J. Kellock, J.E.E. Baglin and E.E .Fullerton, Appl. Phys. Lett. **79**, 1151 (2001).

[35] S. Maat, A.J. Kellock, D. Weller, J.E.E. Baglin, E.E. Fullerton, J. Magn .Magn. Mater. **265**, 1 (2003).

[36] C. Houpert, F. Studer, D. Groult and M. Toulmonde, Phys. Res. B **39,** 720 (1989).

[37] R. Kumar, S.B. Samantra, S.K. Arora, A .Gupta, D. Kanjilal, R. Pinto, A.V.Narlikar, Solid. State. Commun. **106**, 805 (1998).

[38] R. Kumar, S.K. Arora, D. Kanjilal, G.K. Mehta, R. Bache, S.K. Date, S.R. Shinde, L.V. Saraf, S.B. Ogale and S.I. Patil, Radiat. Eff. Defects. Solids. **147**, 187 (1999).

[39] Z.G. Wang, C. Dufour, E. Paumier and M. Toulemonde, J. Phys.: Cond. Mat. **6,** 6733 (1994).

[40] K. Izui, S. Furuno , Proceedings of the 11th International Congress on Electron Microscopy, Kyoto, edited by T. Imura, S. Maruse, T. Suzuki, Jpn Soci. Elec. Mic. Tokyo **1299** (1986).

[41] A. Meftah, F. Brisard, J.M. Costantini, M. Hage-Ali, J.P. Stoquert, F. Studer and M. Toulemonde, Phys. Rev. B **48**, 920 (1993).

[42] F. Thibaudau, J. Cousty, E. Balanzat and S. Bouffard, Phys. Rev. Lett.**67** ,1582 (1991).

[43] Abhishek Kumar, Poonam Kumari, A. Das, G.D. Dwivedi, P. Shahi, K.K. Shukla, A.K. Ghosh, A.K. Nigam, K.K. Chattopadhyay and Sandip Chatterjee , J. Solid State Chem. **208** 120 (2013).

[44] D. Reinen and C. Friebel, Springer-Verlag, Berlin/NewYork. **37** (1979)

[45] R. Kanno, Y. Kawamoto, Y. Takeda, M. Hasegawa, O. Yamamoto and N. Kinomura J. Solid. State. Chem. **96,** 397 (1992).

[46] V.B. Shirokov, Y.I. Yuzyuk, V.I. Torgashev and A.S. Prokhorov, Phys. Solid. State. **47**, 539 (2005).

[47] J. Preudhomme and P. Tarte, Spectro. Acta. A: Mol. Biomol. Spec. **28**, 69 (1972).

[48] J. Ferré, C. Chappert, H. Bernas, J.P. Jamet, P. Meyer, O. Kaitasov, S. Lemerle, V. Mathet, F. Rousseaux and H. Launois, J. Mag. Mag. Mater. **198**, 191 (1999).

[49] J. Juraszek, J. Fassbender, S. Poppe, T. Mewes, B. Hillebrands, D. Engel, A. Kronenberger, A. Ehresmann and H. Schmoranze,r J. Appl. Phys. **91,** 6896 (2002).

50 J. Hamrle, S. Blomeier, O. Gaier, B. Hillebrands, H. Schneider, G. Jakob, B. Reuscher, A. Brodyanski, M. Kopnarski, K. Postava and C. Felser, J. Phys. D: Appl. Phys. **40**, 1558 (2007).

51 D. Schafer, P.L. Grande, L. G. Pereira and J. Geshev, J. Appl. Phys. **109** , 023905 (2011).